On site monitoring during nearby drilling operations toward a geothermal power system installation

Daniele Bortoluzzi*[1a], Sara Casciati[1b], Lucia Faravelli[1b] and Matteo Francolini[3c]

[1] SIART Srl, via dei Mille 73, Pavia, Italy
[3] Formerly SIART Srl, via dei Mille 73, Pavia, Italy

(Received , Revised , Accepted)

Abstract. Among the approaches to the production of "green" energy, geothermal power systems are becoming quite popular in Europe. Their installation in existing buildings requires an extended, external pipes appendix whose laying operation needs a drilling activities nearby structural skeletons often designed to support static loads only, especially when ancient buildings are targeted {#7}. This contribution reports and discusses the experimental results achieved within a specific case study within the European project GEOFIT. In particular, standard accelerometric measurements in and nearby a single-story reinforced concrete building are collected and analysed in the absence of drilling (*pre-drilling*) and during drilling activities (*drilling phase*) to monitor the structure response to the external source of vibrations related to the excavations phase. The target is to outline automatic guidelines toward installations preventing from any sort of structural damage.

Keywords: geothermal power; green-energies; drilling; on site data collection; structural health monitoring;

1. Introduction

The current European Union (EU) policy aims to increase the use of "green" energies within the more than 20 European Countries forming the Union. The goal is to reduce, in the next years, the carbon footprint. Within this strategy, the exploitation of the geothermal energy is a well promising approach. Some technical issues related to the implementation of such a technology limit current applications to isolated buildings far from urban nuclei. The installation itself requires a drilling activity close to the reference building. The source of vibrations caused by drilling activities may result dangerous for the target building (Barrile *et al.*, 2015). Thus, a careful Structural Monitoring (SM) on site, during excavation, is a must to prevent from any sort of structural damage (Kaloop, Mosbeh R. *et al.*, 2020; Ghiasi, Ramin; Ghasemi *et al.*, 2021).

Structural monitoring means to collect data in and nearby an existing building. It is the necessary support for a diagnosis and a prognosis, which together forms a second stage often referred to as Structural Health Monitoring (SHM) (Ye, X.W. *et al.* 2019). SHM refers to the process of implementing a damage detection and characterization strategy for engineering structures such as structures and infrastructures. In these cases, damage is defined as changes into the material and/or the geometric properties of the reference structural system, including changes in the boundary conditions and system connectivity, which can adversely affect the system performance. The SHM process involves observing a system over time using response measurements sampled periodically by a series of sensors (such as accelerometers), extracting damage-sensitive functions from these measurements and statistical analysis of these characteristics to determine the current state of health of the system (Cao, Yan *et al.*, 2020; Zhang, Qilin *et al.*, 2021).

Within the GEOFIT (Deployment of novel GEOthermal systems, technologies and tools for energy efficient building retrofitting, see GEOFIT website) project of the Horizon2020 European Union programme, SM has a central role. Structural monitoring activities in some pilot locations within the Consortium have been carried out to develop a methodology for a rapid building assessment during worksite to avoid any traumatic event (building damage).

In this paper, the results achieved in a pilot case, both in the pre-drilling stage and during the drilling operations, are presented and discussed.

2. The "Sant Cugat" pilot case

When dealing with an existing building, SM has a two-fold role:

i) on one side, its results should check that the installation of a geothermal plant is painless for the target existing building;
ii) on the other side, one expects a deeper understanding in the knowledge of the excitation source, of the soil propagation pattern and of the building signature.

These aspects are conveniently managed when there is the availability of pilot sites.

This is the case of the "Sant Cugat pilot site (Els Pins del Vallès School)" located about 25km North-West of the town

*Corresponding author, Ph.D.
E-mail: danielebortoluzzi.ing@gmail.com
[a] Ph.D.
[b] Professor
[c] Engineer

of Barcelona (Spain) (Casciati *et. al*, 2019). The Pins del Vallès School consists of three reinforced concrete buildings (see Fig. 1):

1. School main building;
2. Administrative building (see Fig. 2);
3. Pavilion building.

Fig. 1 The Pins del Vallès School pilot site

Fig. 2 The administrative building where the tests were carried out

The building investigated during this structural monitoring campaign is the administrative building, i.e., the closest to the selected drilling site.

From a geometric point of view, the building has a rectangular-shaped plan: about 23.70 by 12.75 m. It has only one floor above the ground and a double-pitch roof. The inter-floor height varies in the range from 2.50 to 3.50 m. It basic structural scheme consists of reinforced concrete (RC) columns, beams and walls (see Fig. 2).

3. The experimental campaign

The tests carried out on the administrative building were designed to identify the dynamic behaviour of the building in the original state (pre-drilling) and during the drilling activities. In particular, the survey has been organized as follows:

1. a preliminary investigation aims to determine the current state of the structure. Visual inspection addresses the evaluation of the characteristics of the building in its operational state and the detection of possible anomalies and/or damage.
2. a first survey campaign by acquisition of accelerometric signals under environmental loads assesses the building dynamic behaviour in the pre-drilling phase;
3. a second survey campaign, again by the collection of accelerometric data, covers the drilling phase – i.e., the initial stage of installation of the geothermal energy system. The drilling operations were carried out by a GEOFIT partner different from the writers' company. It was using a standard protocol whose details are not available.

3.1 Monitoring device equipment

The dynamic monitoring system consists of a network of *EpiSensor* high-sensitivity accelerometers (see the Kinemetrics website), able to acquire and record accelerations at different location across the building. Data collection and transmission have been managed by a *Wireless Data Acquisition System (WDAS)* (see Fig. 3) (Casciati, 2011; Casciati, 2012; Chen, 2015; Casciati, 2018).

Fig. 3 Device equipment. WSU means wireless station unit.

3.2 Monitoring campaign

The monitoring campaign was spanning over four different days from July 27th, 2020 to July 31st, 2020. In detail:

- day 1: general inspection to identify evident structural and non-structural damages - if any;
- day 2: data acquisition due to environmental loads (no drilling);
- day 3: the campaign of tests of is completed (no drilling);
- day 4: data acquisition during the drilling activities;

It is worth pointing out that the weather in San Cugat was rather warm during the campaign (about 36-37°C). This slowed down some data acquisition operations and exposed all the electrical devices to hard environmental condition. Furthermore, there were time windows of inactivity due to the presence of students, teachers, etc. inside the pilot site. Therefore, all the monitoring activities were only planned in the early morning and late afternoon.

3.2.1 Day 1 monitoring (July 27th, 2020)

The first day of the monitoring activity is devoted to a preliminary visual inspection of the complex. The aim is to identify the current state of the structure and to evaluate the characteristics of the building in its operational state. One looks for any type of anomalies and damage. The understanding of the dynamic response to environmental actions is important in view of preventing from future structural problems under plant vibrations.

Fig. 4 Site surrounding area (*a*, *b*); main base camp (*c*)

Moreover, this inspection is useful to outline the better way to store the equipment so that it is protected from the action of the sun during the day. Last, but not the least, the inspection activity allows one to identify the best sensor location across the structure (see Fig.4).

This inspection day concluded with the evidence that the administrative building does not present any critical issues regarding to both structural (columns, beams, walls, etc.) and non-structural elements (partitions, countertops, etc.).

3.2.2 Day 2 monitoring (July 28th, 2020)

The first action of the second day of structural monitoring was the selection of a *Cartesian* reference system, which would be retained for the entire period of data acquisitions (*X=horizontal transversal axis; Y=horizontal longitudinal axis; Z=vertical axis*). Four *Episensor FBA accelerometers* were placed on the site. In details, three of these accelerometers (labelled as WS2, WS4 and WS6) were placed near the columns on the long side of the building (*X* direction of the accelerometer reference system), while the device labelled as WS3 was placed on a near manhole (distant one meter from the building wall, see Fig. 5).

The goal of these data campaigns aim to identify the behaviour of the structure at its current state, evaluating the dynamic response under environmental actions.

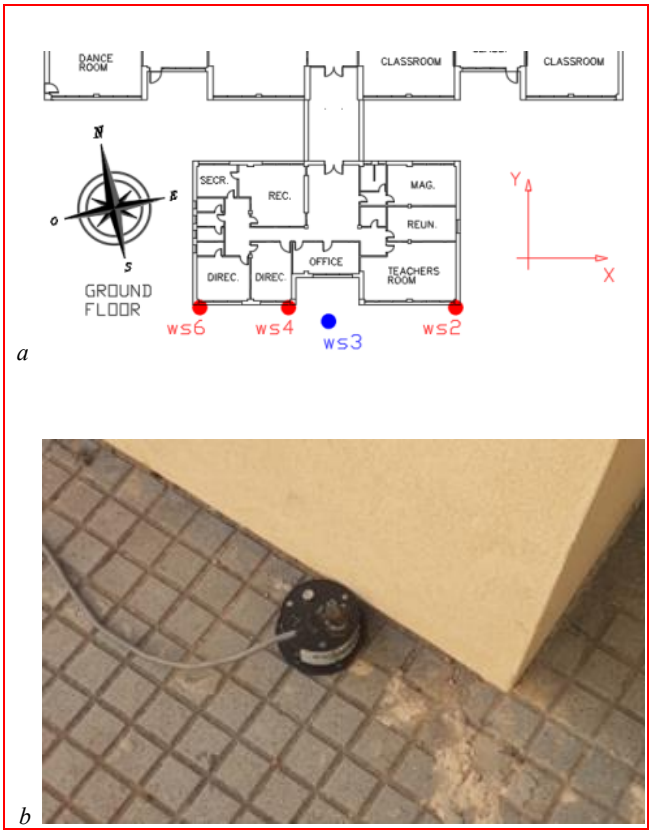

c

Fig. 5 Devices at the ground level along the *X* direction (*a*); WS2 (*b*); WS3 (*c*).

This configuration was defined to better assess the possible vibrations coming from the excavation area, when the drilling would have started. Thus, the same devices configuration was replicated on Friday July 31st, 2020 during the drilling activities. With this device configuration, 3 environmental tests of different duration, spanning from 10 to 25 minutes, were carried out.

3.2.3 Day 3 monitoring (July 30th, 2020)

During the third day of structural monitoring, four environmental tests were performed, setting three accelerometers (WS2, WS4, WS6) along the *Y* direction of the administration building. The selected locations were at the bottom of the columns: the devices labelled as WS2 and WS6 at the ends of the short side of the structure, and the device labelled as WS4 at the centre (see Fig. 6). Four environmental vertical tests were carried out, each of them lasting about 20-30 min.

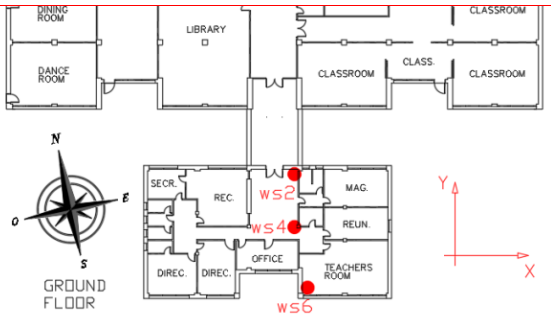

Fig. 6 Devices at the ground level along the *Y* direction

3.2.4 Day 4 monitoring (July 31st, 2020)

The last day of the campaign was also the first drilling day at the GEOFIT pilot site (see Fig. 7).

Fig. 7 Drilling site and operation

The first drilling reached a depth of 60 m on the total of 120 m for each foreseen single hole. The drilling phase lasted from 1:00 p.m. to 3:30 p.m. and, during this time window, the data acquisition on the administrative building proceeded.

During the drilling phase, part of the structural tests carried out on the administrative building during the previous days was replicated. In detail:

- ground level data acquisition with the devices along direction *X* (see Fig. 5);
- ground level data acquisition with the devices along direction *Y* (see Fig. 6).

In addition, in order to identify the drilling-machine working frequencies, a data acquisition test focused on the drilling machine, (see Fig. 8), was carried out by installing an *Episensor FBA* accelerometer directly on the machine. One more remark: data acquisitions on drilling machine have been carried out just switching on the machine without any drilling activities.

Fig. 8 The accelerometer on the drilling machine

4. Elaborations of the recorded signals

This section reports the elaborations from the accelerometric signals collected during the monitoring campaigns.

The data analysis used the tools offered by the *MatLab environment* (see the Matlab website) and plotted in terms of periodograms. One estimates such periodogram in two alternative ways:

a. either by plotting the square of the absolute value of the signal's *Fast Fourier Transform* (*FFT*) multiplied by the time step (0.01s for all the recorded signals) and divided by the numbers of recorded points. The covered frequency range is from 0 to 50Hz, for a time step of 0.01s, and the frequency step results from the division of the higher frequency value, 50, divided by one half of the number of available recording times.
b. or by estimating the power spectral density of the signal for a given frequency step.

Option "a" was used to obtains the plots in Figure 9, mainly due to the wish of exploiting the entire reliable parts of the recorded signals and the goal of checking possible discrepancies in the results. Discrepancies that in Figure 9 are quite insignificant.

In section [3.2] option "b" was selected by adopting a discretization of the range 0-50 Hz in 512 points. This scheme works on windows of the signal of 1024 points and keep the mean over the available windows. To preserve the same degree of accuracy not the entire signals are compared but segments of the same length, made of 1024 points, i.e., 2 to power 10. In particular, segments of length 32,768 (2^15) were retained.

All recorded data have been gathered in terms of "*Volts*" and then converted into acceleration "m/s^2" simply multiplying "Volts" by the factor "1/2.5" according to the technical specification of the accelerometers. In the plots of Figures 9, 11, 12, 13 and 15, the ordinates are still in [V^2/Hz]. One more remark applies. When using wireless sensor units for the data transmission and collection – as done in this case study (see section [2.1]) – there is the risk that some data are lost in the transfer. The workstations adopted in the test come with the option of storing not only the received data but also the history of the transmission. This allows the operator to detect if data lost occurred as well as if some workstations received more points than others did. Therefore, in selecting the test among the several replicates carried out at the same sensor locations, the criterion of having the same number of recorded points was adopted. In other words, the elaborations cover reliable data only.

4.1 Dynamic characterization of the drilling machine

Consider first the signals collected having the drilling machine as direct source by installing an *Episensor FBA* accelerometer directly on the machine according to Fig. 8. The recorded signals are quite dense and homogeneous and span between -0.3V and 0.2V, (with zero mean) in the *X* direction, and between -0.2V and 0.3V in the *Z* direction (with zero mean). The former one shows divergence (resonance). Along the *Y* direction, only noise is detected.

The periodograms along direction *X* and Z are shown in Figure 9. These results show how the drilling machine itself generates three main frequencies around 13 Hz, 28 Hz and 43 Hz.

4.2 Signals elaboration pre- and during drilling phase

One move now to the results of the signal elaborations coming from the structural monitoring campaigns planned and developed as explained in sub-sections [2.2.2], [2.2.3] and [2.2.4].

The main goal of this step is to assess a comparison between the signals recorded during drilling phase and the signals recorded in the absence of any excavation activity.

To facilitate the comparison, the data are plotted separately for the two cases of devices placement along the *X* direction and the *Y* direction (see sub-sections [2.2.2] and [2.2.3]).

4.2.1 Administrative building results – sensors configuration along the X direction

The first sequence of results plotted refers to the placement of the devices along the *X* direction as sketched in Figure 10.

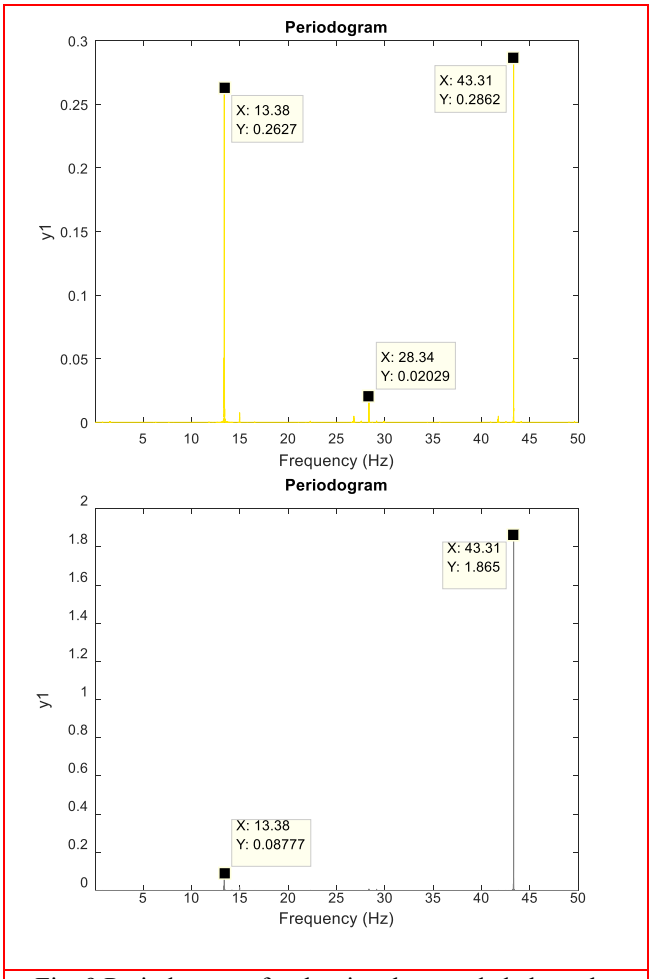

Fig. 9 Periodograms for the signals recorded along the directions *X* (top) and *Z* (bottom).

For any selected set of data, the mean is first removed. Then a band-pass filter covering the window 0.8 – 50 Hz filters the signal. The plots give the periodograms achieved by a Power Spectral Density (*PSD*) estimate on windows of 2^10 (=1,024) points.

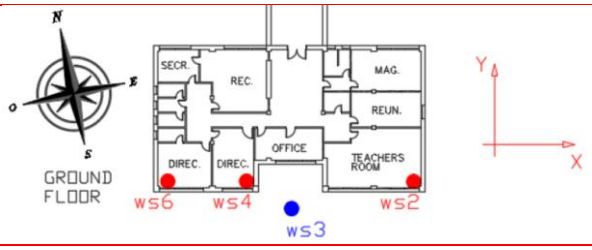

Fig. 10 Devices configuration - *X* direction

The data plotted in Figure 12 come from the elaboration of the data recorded at WS3 along directions *Z* and *X*. The left column covers the "pre-drilling" tests (sections [2.2.2] and [2.2.3]); the right column those during the drilling activities (section [2.2.4]).

Figures 13 and 14 shown the elaborations of the data collected by the other workstations (WS1, WS4 and WS6) for the components along directions *Z* and *X*, respectively. In particular: the left columns cover the Power Spectral Density (*PSD*) for the data coming from the "pre-drilling" tests (sections [2.2.2] and [2.2.3]); the right columns show the Power Spectral Density (*PSD*) for the collected data during drilling activities (section [2.2.4]).

The plots on the r.h.s. of Figure 12 give evidence that the incoming signal is much more rich in frequencies than those reported in Figure 9 at the source, but without any soil penetration. Thus, the populated range of frequencies could be simply caused by the drilling advance or by a more complex soil filtering. This situation justifies the selection of the manhole location as site external to the building able to detect the real incoming signal.

It is worth noticing that, despite the pretty environmental excitation, peaks could be detected in the plot on the l.h.s. of Figure 11. This cannot be the effect of the geothermal system, which has still to be installed, nor of ongoing visible activity. The road traffic if far enough from the sensors. Nevertheless, the values of the peaks is negligible when compared with those on the figure r.h.s.

4.2.2 Administrative building results – Y sensors configuration

The second sequence of data to be elaborated corresponds to the placement of the devices along direction *Y* as sketched in Figure 11.

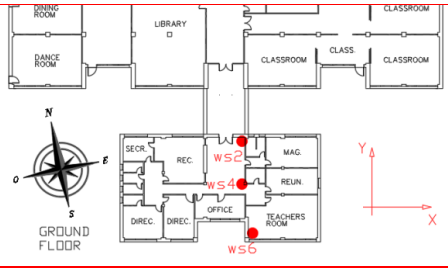

Fig. 11 Devices configuration - *Y* direction

For any selected set of data, the mean is first removed. Then a band-pass filter in 0.5-5 0Hz filters the signal. The following plots report the periodograms achieved by a Power Spectral Density (*PSD*) estimate on windows of 2^10 (=1,024) points.

Figures 15 shows the elaborations of the signals collected by the workstations labelled as WS1, WS4 and WS6 for the components along *Z* direction. In particular: the left columns cover the Power Spectral Density (PSD) for the data coming from the "pre-drilling" tests (sections [2.2.2] and [2.2.3]); the right columns show the Power Spectral Density (PSD) for the collected data during drilling activities (section [2.2.4]).

4.3 Conclusive remarks

As a first conclusion from the data that have been gathered, managed and discussed above, the intensity of the vibration induced by the drilling was low enough to prevent from having any sort of damage. Even if low weight and loosened non-structural elements such as window frames, doors, connections, joints, interior pipelines, furniture and so on can easily be effected within driving high frequencies collected on site, especially for long durations of drilling activities, the intensity of the vibration induced by the drilling was low enough to prevent from having any sort of damage in the building under study. Nevertheless, there are two acceleration components that have to be followed in their path from the source (the drilling machine) to the building to be equipped with the designed geothermal system. The drilling machine itself generates three main frequencies, but only the intermediate one, around 28 Hz, is detected in Figure 12 in both the plots, associated with the *X* and *Z* directions, respectively. The higher value (43 Hz) is only preserved in the *Z* direction. As always occurs when the tests are associated with events that do not admit replicates, one feels the need of a unthinkable deeper supplement of investigation answering to two main questions:

a) which is the cause of the differences in the values of the manhole when compared with the values recorded on the drilling machine? Is it the effect of the soil filtering? Is it the result of the contrasting soil penetration by the machine tool
b) the low value is it generated by the second frequency at the drilling machine or is it the harmonic of the first frequency at the drilling machine?

Even without answering these two questions, the workstation on the manhole shows that there is an external input when the drilling machine is active, input that was absent in the previous days. The signals, when moving from the drilling site up to the ground level where the school is located, decay with the frequency at 28 Hz remaining dominant. From the manhole, one can now move to the basement of the administrative building. Figure 13 explains that the WS6 is receiving along the vertical direction a signal of the same intensity of that at the manhole, while this component decays along the direction *X* from WS6. The same message comes from Figure 14 about the acceleration component along direction *X*. The vertical signal at the manhole preserves its intensity at WS6 in Figure 15, decays quickly in WP4 but regain intensity in WS1.

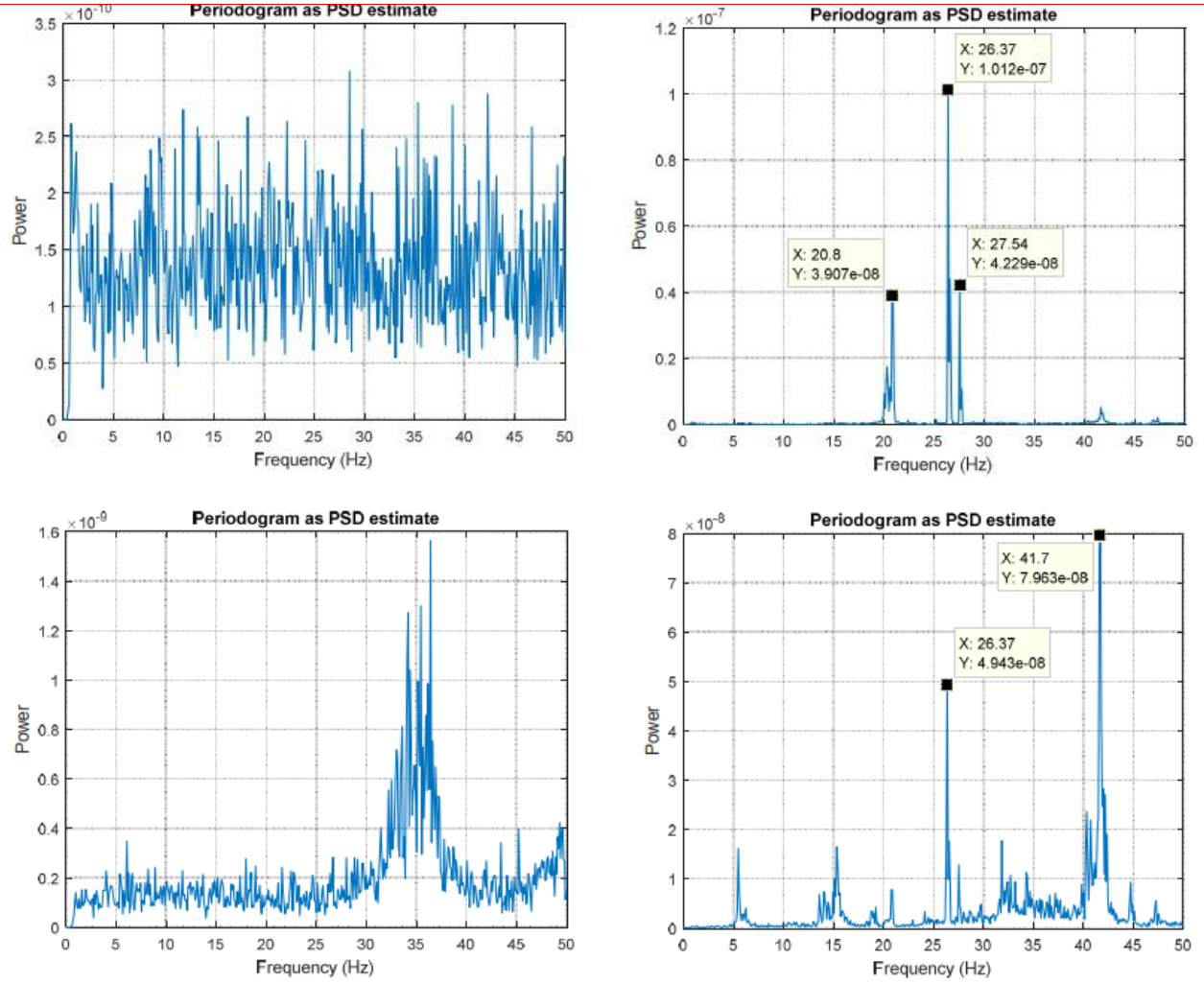

Fig. 11 PSDs of the signals collected at the workstation WS3 along directions *X* (top) and *Z* (bottom): left "pre-drilling"; right "during the drilling"

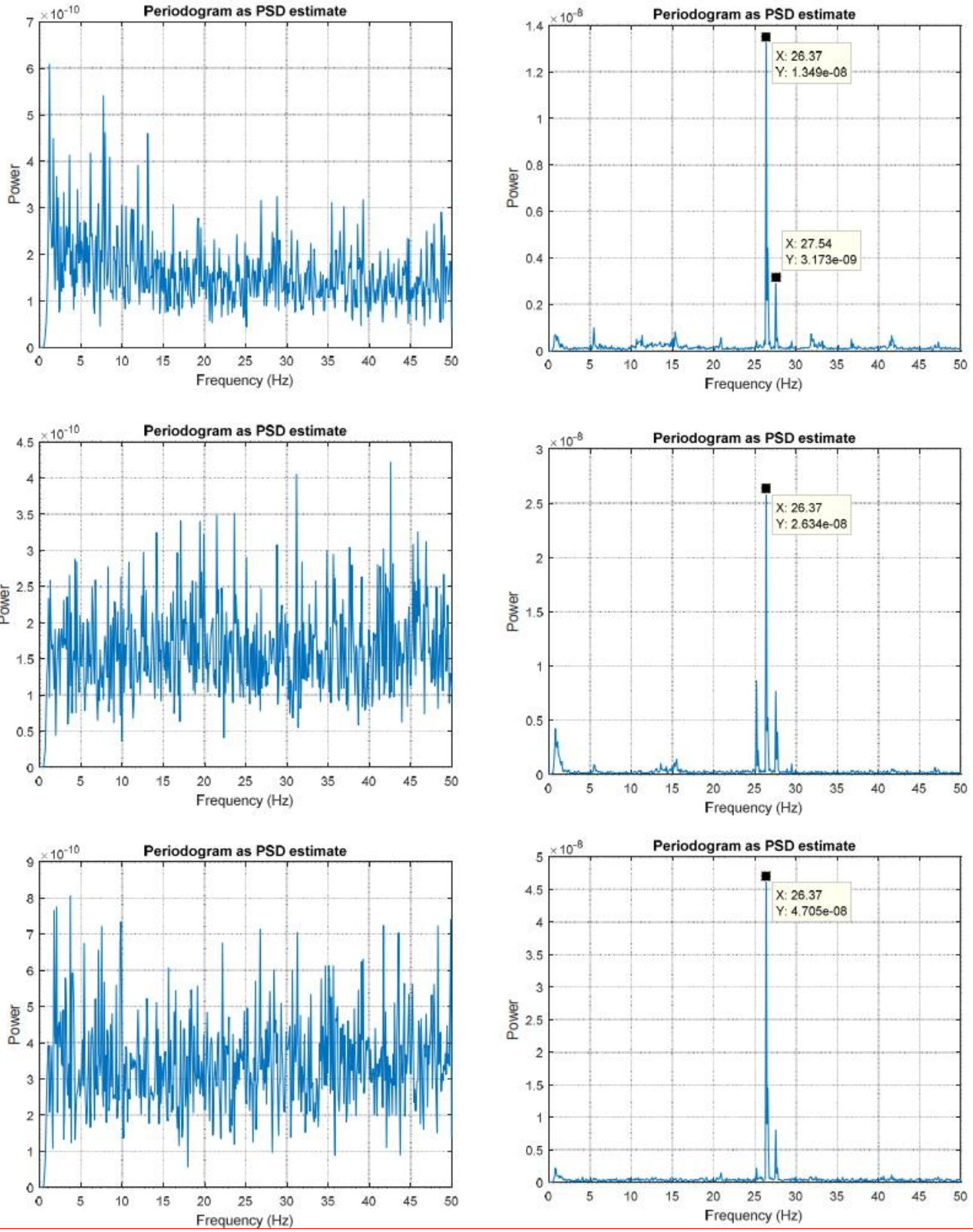

Fig. 12 PSDs of the signals collected along directions *Z* signals at the workstations WS2 (top), WS4 (middle), WS6 (bottom): left “pre-drilling”; right “during drilling”

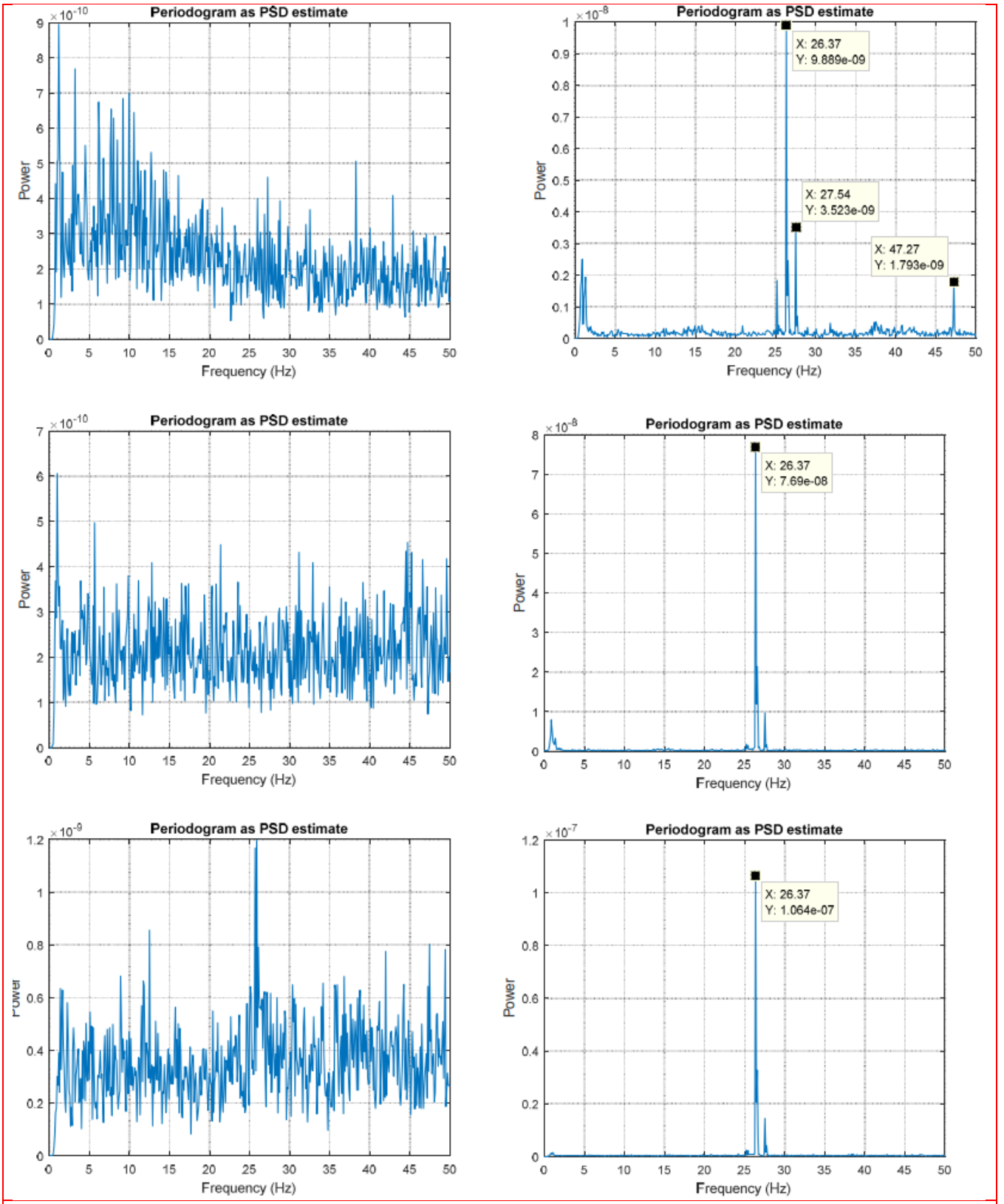

Fig. 13 PSDs of the signals collected along directions *X* at the workstations WS2 (top), WS4 (middle), WS6 (bottom): left "pre-drilling"; right "during drilling"

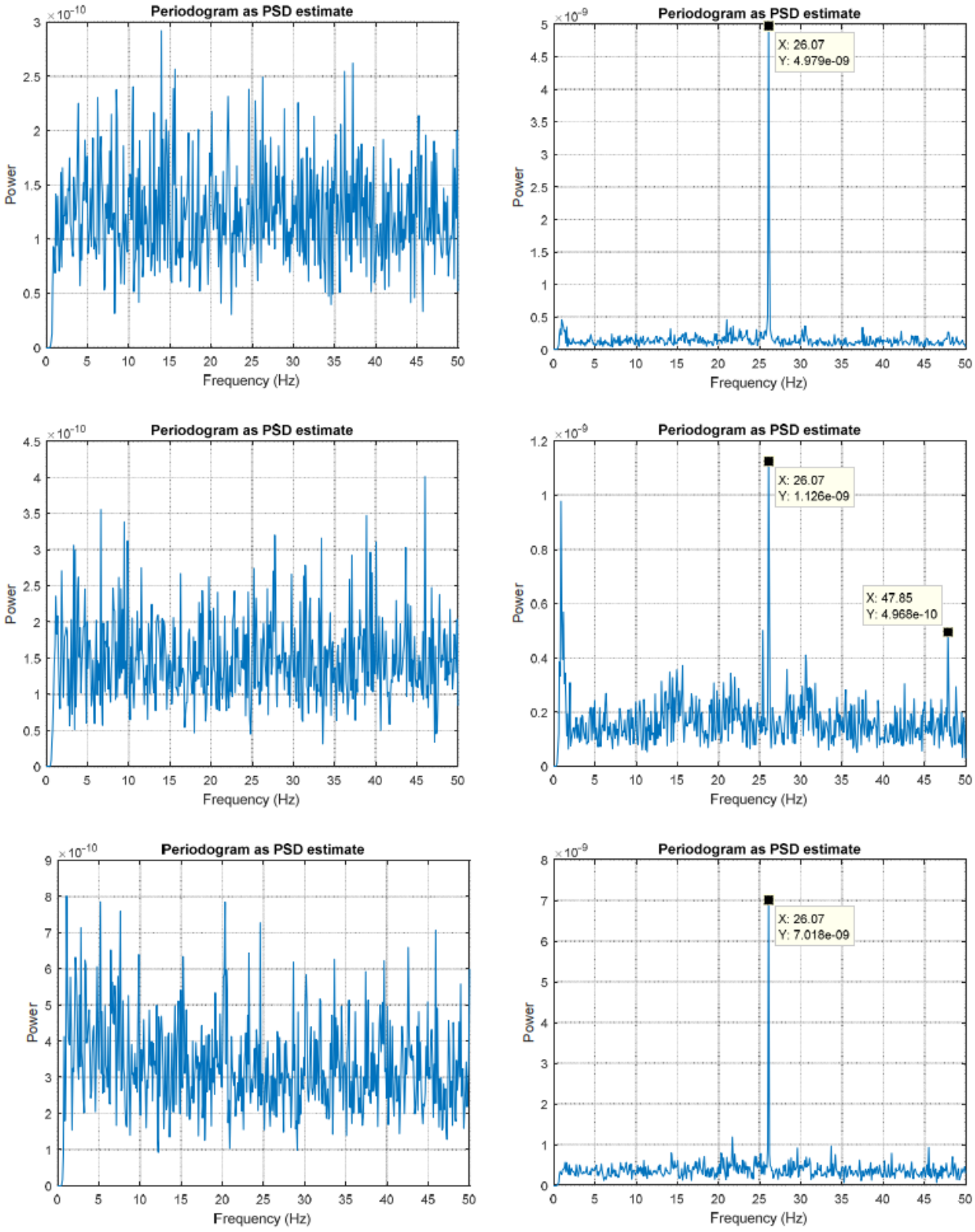

Fig. 15 *Z* signals PSD. WS1 (top), WS4 (middle), WS6 (bottom): left “pre-drilling”; right “during drilling”

5. Conclusions

In this paper the data collection, and their elaborations, of some tests on a RC single-story building located in San Cugat (Barcelona-Spain) have been presented and discussed. In particular, the collected data cover the pre-drilling and the drilling stages.

As a first step, in this monitoring campaign, the building has been visually inspected to evaluate its characteristics and to search for any anomalies and damage. Then a dedicate monitoring campaign based on the acquisition of acceleration data of sensitive points along the structures under environmental loads and under drilling activities has been designed and implemented.

From this experience of the pilot case, one could extract the following items in view of guidelines for an automatic implementation of a geothermal power system in an existing building:

a) define the "drilling machine";
b) test the propagation of the vibration from the drilling location to the existing building;
c) replicate the test at different depth of excavation, to understand the different response at the basement;
d) produce the building signature to identify the frequencies sensible to nearby vibrations.

The whole process could easily be implemented in a consultation assistant. It would allow to use in the field technicians in thermos-technique also without any background in vibration mechanics.

Acknowledgments

The activity reported in this paper has received funding from the *European Union Horizon 2020* research and innovation program under grant agreement **No 792210** (Geofit).

References

V. Barrile, G. Bilotta, D. Lamari, G. M. Maduri, U. Monardi Trungadi e A. Ricciardi, "Computer vision/structure for motion per la diffusione dei beni culturali (in Italian)" in *Proceedings of XIX Conferenza Nazionale ASITA*, Lecco, 2015.

Kaloop, Mosbeh R. ; Elsharawy, Mohamed; Abdelwahed, Basem; Hu, Jong Wan; Kim, Dongwook. "Performance assessment of bridges using short-period structural health monitoring system: Sungsu bridge case study". Smart Structures and Systems. Volume 26 Issue 5 / Pages.667-680 / 2020 / 1738-1584(pISSN) / 1738-1991(eISSN) - Techno-Press

Ghiasi, Ramin; Ghasemi, Mohammad Reza; Chan, Tommy H.T. "Optimum feature selection for SHM of benchmark structures using efficient AI mechanism". Smart Structures and Systems - Volume 27 Issue 4 / Pages.623-640 / 2021 / 1738-1584(pISSN) / 1738-1991(eISSN) - Techno-Press

Ye, X.W.; Jin, T.; Yun, C.B. "A review on deep learning-based structural health monitoring of civil infrastructures". Smart Structures and Systems - Volume 24 Issue 5 / Pages.567-585 / 2019 / 1738-1584(pISSN) / 1738-1991(eISSN) - Techno-Press

Cao, Yan; Miraba, Sepideh; Rafiei, Shervin; Ghabussi, Aria; Bokaei, Fateme; Baharom, Shahrizan; Haramipour, Pedram; Assilzadeh, Hamid. "Economic application of structural health monitoring and internet of things in efficiency of building information modelling". Smart Structures and Systems - Volume 26 Issue 5 / Pages.559-573 / 2020 / 1738-1584(pISSN) / 1738-1991(eISSN) - Techno-Press

Zhang, Qilin; Sun, Siyuan ; Yang, Bin; Wuchner, Roland; Pan, Licheng; Zhu, Haitao, "Real-time structural health monitoring system based on streaming data". Smart Structures and Systems - Volume 28 Issue 2 / Pages.275-287 / 2021 / 1738-1584(pISSN) / 1738-1991(eISSN) - Techno-Press

F. Casciati, S. Casciati, A. Colnaghi and L. Faravelli, "Geothermal Power: Monitoring the Building Response During Installation," in *Proceedings IWSHM*, Stanford, California, USA, 2019.

S. Casciati, Z. Chen. 2011. "A multi-channel wireless connection system for structural health monitoring applications" *Structural Control & Health Monitoring*, Volume: 18 Issue: 5 Pages: 588-600.

S. Casciati, L. Faravelli, Z. Chen. 2012. "Energy harvesting and power management of wireless sensors for structural control applications in civil engineering" *Smart Structures and Systems*, Volume: 10 Issue: 3 Pages: 299-312.

Z. Chen, S. Casciati, L. Faravelli. 2015. "In-Situ Validation of a Wireless Data Acquisition System by Monitoring a Pedestrian Bridge" *Advances in Structural Engineering*, Volume: 18 Issue: 1 Pages: 97-106.

F. Casciati, S. Casciati, M. Vece. 2018. "Validation range for KF data fusion devices" *Acta Mechanica*, Volume: 229 Issue: 2 Special Issue: SI Pages: 707-717

GEOFIT website, https://geofit-project.eu

KINEMETRICS, https://kinemetrics.com

MATLAB, https://www.mathworks.com